

Design of Sabo Dam at Sapang Maeyag as Creek, Along Barangay San Juan Baño, Arayat, Pampanga

Avy Danielle G. Rodriguez*, Melany B. Santos**, Gillian T. Roxas***, Veronica Anne L. Samson****, Rica Mae S. Serrano *****, Cyrus A. Rizare*****, Jayrenzo Matthew S. Soriano*****

*Department of Civil Engineering, Don Honorio Ventura State University, Bacolor, Pampanga, Philippines
Email: avydaniellerodriguez651@gmail.com

**Department of Civil Engineering, Don Honorio Ventura State University, Bacolor, Pampanga, Philippines
Email:santosmelanyb@gmail.com

***Department of Civil Engineering, Don Honorio Ventura State University, Bacolor, Pampanga, Philippines
Email: gillianroxas1127@gmail.com

****Department of Civil Engineering, Don Honorio Ventura State University, Bacolor, Pampanga, Philippines
Email: veronicasamson13@gmail.com

*****Department of Civil Engineering, Don Honorio Ventura State University, Bacolor, Pampanga, Philippines
Email:imricamaeserrano@gmail.com

*****Department of Civil Engineering, Don Honorio Ventura State University, Bacolor, Pampanga, Philippines
Email:cyrusrizare17@gmail.com

*****Department of Civil Engineering, Don Honorio Ventura State University, Bacolor, Pampanga, Philippines
Email:jayrenzomathewsoriano@gmail.com

Abstract:

Debris flow, driven by gravity, moves water, air, and debris rapidly across vast distances, causing significant harm to humans, homes, infrastructure, and the environment. Sabo dams, or debris retention dams, are essential for managing sediment-related risks like landslides, debris flows, and floods in mountainous areas. This study evaluates their effectiveness at SapangMaeyagas Creek, San Juan Baño, Arayat, Pampanga. The study assessed Sabo dams for debris trapping ability, structural strength, and societal or environmental impacts. Data on peak discharge and hydraulic flow depth analysis guided the design for safety, efficiency, and sustainability, ensuring effective debris flow management with minimal adverse impacts. The study confirmed the Sabo Dam's safety and strength against failures such as overturning, sliding, and bearing capacity. Researchers determined specific values: discharge rate (31.4 m³/s), hydraulic depth (0.52m), maximum depth (8m), width (20m), and velocity (5.6m/s) of debris flow. These findings informed the design of a capable Sabo Dam. This thesis enhances Sabo dam technology, providing a framework for designing and upgrading debris flow control structures in mountainous areas, focusing on sustainability and community resilience.

Keywords —Debris flow, Sabo Dams, Debris Retention, Hydrological studies, Hydraulic Analysis

I. INTRODUCTION

A. Debris Flow

Debris flow is an inherent natural occurrence characterized by significant destructive potential, mostly influenced by the force of gravity. It is comprised of a combination of water, air, and

debris, rendering it as one of the most destructive forms of mass movement due to its notable flow velocity and extensive travel distances. Debris flows have been responsible for significant societal, human, residential, infrastructural, and environmental impacts on a global scale [1].

They which occur frequently in mountainous regions, are considered to be one of the most hazardous and unpredictable types of landslides. They involve the sliding down of wet masses of rock and soil from mountain slopes, followed by their concentration into channels and the deposition of thick, muddy material in valleys. Mountain communities are at a heightened risk of encountering debris flows [2]. For practical reasons and economic considerations, they prefer to stay in these locations. Thus, debris-related disasters have resulted in more human deaths and livelihood losses.

B. Sabo Dams

Sabo Dams, which are considered to be excellent structural interventions for the management of debris flow, play a significant role in mitigating the impact of such natural phenomena. In recent years, numerous researchers have conducted tests pertaining to the optimal functioning of Sabo Dams, which exert significant influence on both ecological and landscape aspects. These dams are additionally subjected to the impulsive stresses exerted by debris flows. This is evident in the longitudinal section of a debris flow, where the front portion is particularly significant and intricate due to the accumulation of sizable stones. The mitigation of energy in the leading section of a debris flow is crucial for safeguarding the downstream region due to the significantly heightened destructive potential exhibited by debris flows in comparison to clear fluids. Hence, it is imperative to conduct a thorough examination of the mechanisms underlying debris flows in relation to diverse Sabo Dams, with the aim of mitigating debris-related disasters [3].

C. Types of Sabo Dams

The manual titled Technical Guideline for Designing Sabo Facilities against Debris Flows and Driftwood [4] explains the methods for designing facilities to minimize the impact of debris flows and driftwood, as required by the Sabo master plan. This master plan is formulated based on the principles outlined in the Technical Guideline for Establishing Sabo Master Plan against Debris Flows and Driftwood [5].

According to the guideline, there are three types of openings of Sabo Dams, namely open type, semi-open type, and closed Sabo Dams. This

section contains the parameters in order to determine the appropriate type of Sabo Dam opening.

The evaluation of the kind of Sabo Dam was conducted based on the results of a field survey, taking into account the characteristics of the target region, the anticipated event, the economic efficiency, and the environmental conditions of the site.

The main purpose of Sabo Dam is to prevent the occurrence of debris flows in the source and scouring zone. However, if the dam is built in a transport or deposition zone, it must primarily serve the following functions:

- Capturing debris flow
- Maintain the space corresponding to the design capturing volume of debris flow
- Conserve the river environment at normal times (continuity of the river)

Closed Type Sabo Dams

Maintain the torrent bed and contain debris flow

- Stabilize channel side slopes to reduce scour, capture debris, and reduce flow speed
- Retain coarse particles and fine materials
- Intercept debris flow downstream

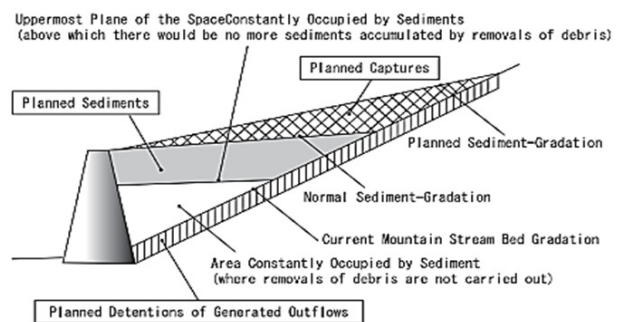


Fig. 1 Debris to be computed in the management plan for debris flows for closed-type

A Sabo Dam that is either open or semi-open should be constructed in a way that the open part is fully obstructed by big stones, boulders, or similar materials. This is necessary to ensure that the dam can effectively contain the expected amount of debris flow. Furthermore, the spatial arrangement of this type of dam should take into account the pattern of debris transport.

Open Type Sabo Dams

- Constrain the flow of a channelized debris flow
- Trap medium to large size debris (e.g., rocks, boulders, driftwood and debris)
- More compatible with the natural environment

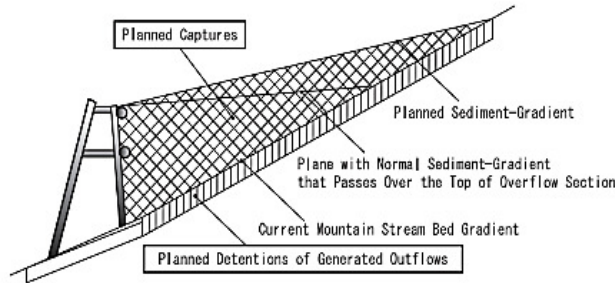


Fig. 2 Debris to be computed in the management plan for debris flows for open type

Open and Semi-Open Type Sabo Dams

- Capture debris flow as the boulders carried by the debris flow blocks its open section
- Dam allows harmless debris to flow downstream normally
- Enough capacity to trap debris flow because they normally allow debris to pass through

Additionally, the semi-open format may be utilized in the situations listed below:

- It is expected that fine particle of debris is dominant
- Low debris concentration is expected due to gentle slope
- Muddy water due to flooding (other than debris flow) near the mouth of valley needs to be directed to downstream channel

Fig. 3 Debris to be computed in the management plan for debris flows for semi-open type

D. Loads on Sabo Dam

The weights acting on a Sabo Dam encompass various factors, including self-weight load, hydrostatic pressure, deposited debris pressure, debris flow fluid force, rock impact load, and uplift pressure [6, 7, 8].

Self-Weight Load

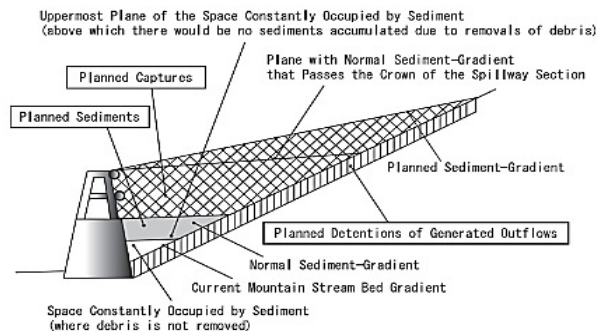
The magnitude of the dam's weight, along with that of its foundation, constitutes a significant counteracting force. The calculation involves the multiplication of the volume of the dam, which is determined by the product of its area and a constant value of 1, with its density.

Hydrostatic Pressure

When an object is immersed in a stationary fluid, the fluid pressure generates hydrostatic forces on its outer layer. The perpendicular orientation of these forces is necessary due to the absence of any shear action. Determining these forces involves integrating the static pressure distribution over the corresponding area of being acted upon.

Debris Flow Fluid Force

A debris flow can be described as a flow consisting of solid and liquid phases. The composition and gradation of the particles present within it dramatically influences the impact force of a debris flow. The magnitude of the impact force is intricately linked to several factors, including the volumetric fraction of solid particles, the nature of these particles, the velocity at which they are in motion, and the depth of the debris flow. The boulder impact force is the most significant component of the overall impact force, with the impact force of coarse particles being the second



Typhoon Karding hit on September 25, 2022, residents noticed an expansion of a crack on Mt. Arayat, raising concerns about a potential massive landslide, as highlighted by the PDRRMO [10].

Residents in Purok 4, 5, 6, and 7 of San Juan Baño are directly at risk. A 2014 survey led by MGB's chief geologist Noel Lacadin revealed significant rock displacement since Tropical Storm Ondoy in 2009, with volumes reaching 66,105.60 cubic meters by 2013. Super Typhoon Karding and Severe Tropical Storm Paeng added 4,120 and 1,125 cubic meters of rocks, respectively, totaling 71,350.60 cubic meters by November 2022, equivalent to about 3,963 truckloads [11, 12].



Fig. 4 Aftermath of Typhoon Ondoy with 12 Casualties [9]

In November 2022, Secretary of Public Works Manuel Bonoan approved P100 million for engineering interventions, including debris flow barriers along SapangTakwi, SapangMadalumdum, Sapang Oliva, and SapangMaeyagas. The MGB reported 324,043 cubic meters of erodible materials in the creeks post-typhoons. Additional recommendations include slope protection, risk area delineation, early warning devices, evacuation, dredging, drainage maintenance, and clearing creeks. Long-term solutions, such as Sabo Dams, are also being considered to mitigate risks [13, 14].

F. Rationalization for the Necessity of Constructing the Sabo Dam at Mt. Arayat

Constructing a Sabo Dam at Mt. Arayat is essential due to persistent landslide threats. A significant fissure on the mountain, worsened by Typhoon Karding in September 2022, raises concerns about potential landslides. The PDRRMO warns that another powerful cyclone could trigger a massive landslide, endangering multiple villages. Despite being in a declared danger zone, residents of Barangay San Juan Baño resist relocation, highlighting the need for improved early warning systems. Harmful farming practices like slash-and-burn, as noted by Governor Lilia Pineda, exacerbate soil degradation and erosion, increasing landslide risks. The Mines and Geosciences Bureau confirmed that loose soil and debris worsen river siltation and forest denudation, intensifying flooding during disasters [15, 16].

Reforestation efforts by SCPW and Holcim PH are crucial for protecting the watershed and local ecosystems. These initiatives aim to restore the mountain's ecological integrity, reduce erosion, and support sustainable livelihoods for local farmers. A Sabo Dam is vital for controlling debris flow, safeguarding communities, and preserving the natural environment [17].

G. Statement of the Problem

The study aims to design a Sabo dam for SapangMaeyagas Creek on Mt. Arayat, San Juan Baño, Arayat, Pampanga. The dam will manage and contain harmful debris flow to protect nearby communities. Additionally, the study will assess the dam's safety against potential failure modes.

Specifically, this research aims to answer the following questions:

1. What kind of Sabo Dam is suitable given the specific conditions found on Mt. Arayat based on the Technical Guideline for Establishing Sabo Master Plan against Debris Flows and Driftwood?
2. What are the appropriate design considerations and hydraulic parameters for ensuring the safety of the Sabo Dam in the designated area considering:
 - a. Hydrologic Analysis
 - b. Hydraulic Analysis
 - c. Debris Transport Analysis

3. Does the Sabo Dam fulfill the requirements associated with potential failure modes concerning its external stability?

- a. Stability against shearing
- b. Stability against overturning
- c. Soil bearing capacity

H. Objectives

General Objective:

The study aims to create a comprehensive design for a Sabo dam that is intended to be constructed at the SapangMaeyagas Creek on Mt. Arayat, particularly along San Juan Baño, Arayat, Pampanga. The primary objective of this proposed dam is to function as an infrastructure system that manages and holds back harmful debris flow in the area, thereby minimizing the risk of damage to the surrounding communities. In addition, the study aims to evaluate the safety of the dam against various potential failure modes.

Specific Objectives:

Specifically, this research aims to determine the following:

1. Identify the appropriate type of Sabo Dam by taking into account the conditions present on Mt. Arayat based on the Technical Guideline for Establishing Sabo Master Plan against Debris Flows and Driftwood.
2. Determine the suitable design and safe hydraulic dimensions of Sabo Dam in the selected area based on hydrologic analysis, hydraulic analysis, and debris transport analysis.
3. Assess the External Stability of the Structure with Respect to Sliding, Overturning, and Bearing Capacity Failure.

I. Significance of the Study

Growing evidence indicates a global rise in debris-related disasters due to adverse weather changes and environmental degradation. Structural methods have proven effective in mitigating these disasters. This study aims to design Sabo Dams to safeguard human life and infrastructure, particularly benefiting San Juan Baño, Arayat, against natural events like typhoons.

Key stakeholders include:

Local Government Units (PDRMO and MGB)

They can use the study's data and insights to enhance their expertise and assess the effectiveness of Sabo Dams in protecting communities.

Flood Control and Sabo Engineering Center (DPWH) and other agencies (DA-NIA, DA-BSWM, NPC)

They can evaluate and build Sabo Dams to manage natural resources and secure community well-being.

Communities near landslide-prone areas

The research provides crucial debris flow and flood mitigation strategies, benefiting not only San Juan Baño but also other vulnerable communities.

Residents of San Juan Baño, Arayat

The study offers customized strategies to enhance community resilience and safety for the 1,531 households at risk from Mount Arayat's debris flows.

Future Researchers

The study adds to existing knowledge, offering a framework and reference for future research on Sabo dam analysis and design.

J. Scope and Delimitations

- The study aims to design a Sabo dam at SapangMaeyagas Creek on Mount Arayat, San Juan Baño, Arayat, Pampanga, ensuring stability and safety.
- It focuses on managing debris flow to protect downstream areas. The quantitative methodology assesses the dam's performance and response to failure modes.
- The study addresses debris flows, excluding driftwood, motivated by historical large boulder debris flows on Mt. Arayat.
- Calibration used rainfall data from Typhoon Santi due to the absence of an observed hydrograph.
- The study classifies loads on Sabo dams into Load level 1 (100-year rainfall events) and Load level 2 (200-year debris flow events), using a 100-year interval due to limited data.
- Hydraulic analysis considered steady and non-uniform water flow.
- It focuses on a single dam design, without addressing future maintenance.

K. Conceptual Framework

The conceptual framework shown in Figure 5 is vital for this study's success. Initially, identifying the debris flow path is crucial for determining the optimal location for installing the Sabo Dam. Various computations and analyses, including hydrologic, hydraulic, and Debris Transport Analysis, are conducted to design an appropriate Sabo Dam. Evaluation of the dam's external stability against shearing, overturning, and soil bearing capacity ensures it can withstand potential deformations. This comprehensive approach guarantees the Sabo Dam meets required safety and performance standards.

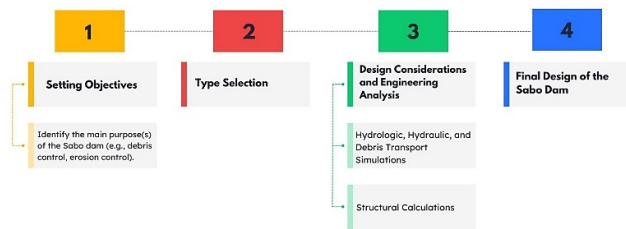


Fig. 5 Conceptual Framework

II. METHODOLOGY

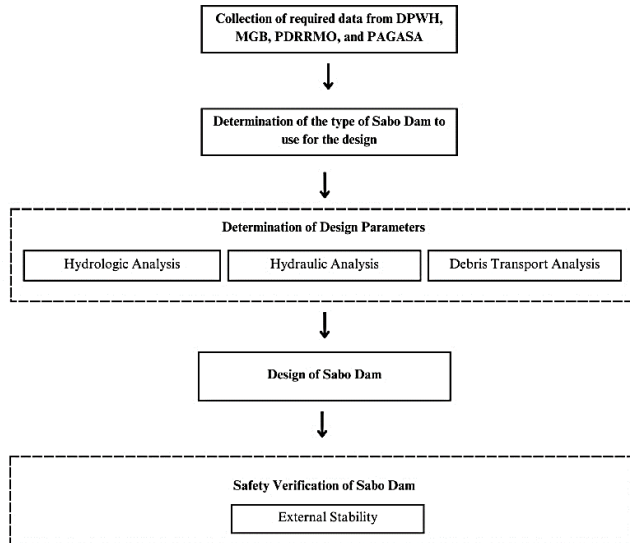


Fig. 6 Methodological Framework

A. Research Design

This research study uses a quantitative approach to systematically collect and analyze numerical data. The case study design focuses on SapangMaeyagas

Creek on Mt. Arayat, the proposed site for the Sabo Dam. While case studies often use qualitative methods, this study employs quantitative methods. Data collected were entered into simulation software for hydrologic, hydraulic, and debris transport analyses, which informed the Sabo Dam design. Detailed calculations were then conducted to validate the dam's structural integrity and resistance to potential failure modes.

B. Research Locale

Sabo Dams are typically built in mountainous areas with abundant bulk materials and high-intensity rainfall. This study focuses on Mt. Arayat, specifically SapangMaeyagas Creek leading to Barangay San Juan Baño, the proposed site for a Sabo Dam. A site investigation was conducted on November 10, 2022, by the Mt. Arayat task force, comprising various regional government organizations. The investigation was prompted by erosional processes during Typhoon Karding, raising concerns among residents about a recurrence of the 2009 landslide that caused fatalities and property loss. The primary aim was to develop preventive engineering strategies to safeguard residential areas from future geological hazards [18].

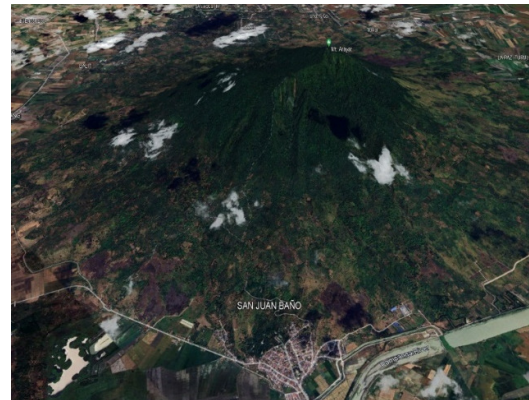


Fig. 7 Photo of Mt. Arayat from Google Earth Pro

C. Research Instrument

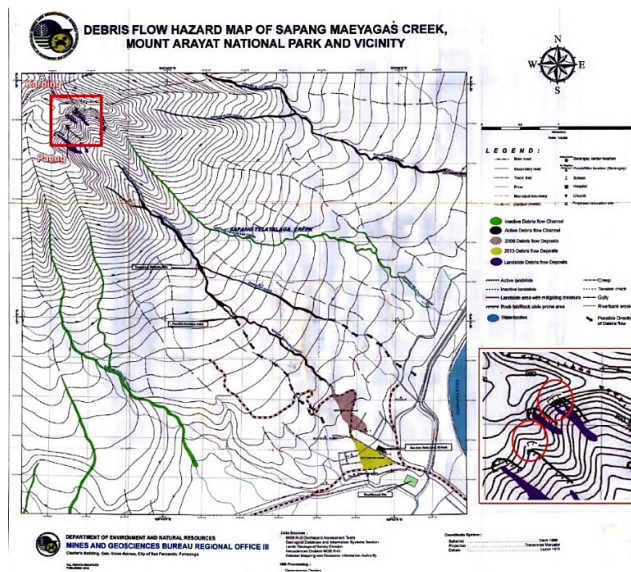
Secondary research uses pre-existing data collected by other researchers. This study utilized data from government agencies such as DPWH, MGB, PDRRMO, and PRFFWC-PAGASA, which included landslide and multi-hazard maps, elevation maps, geotechnical analyses, rainfall maps, and

drone survey reports. These data were essential for analyzing and designing the Sabo Dam. Additionally, software like HEC-HMS and HEC-RAS for hydrologic and hydraulic analysis, and iRIC for debris transport analysis, were employed. Section 2.7 discusses each software's role in data analysis.

D. Data Collection Methods

With the necessary secondary data in hand, the research study progresses towards analyzing and designing a Sabo Dam as a robust engineering solution against debris flow. Data from DPWH, MGB, PDRRMO, and PRFFWC-PAGASA formed the basis of this study, obtained through formal requests accompanied by a letter signed by group members and authorities. Moreover, the internet provides ample relevant information for Sabo Dam design, drawing from diverse online sources like websites, databases, archives, and academic journals. Table I summarizes crucial data collected from government departments, each contributing significantly to the research's overall understanding and analysis.

TABLE I
DATA COLLECTED FROM DIFFERENT GOVERNMENT ORGANIZATIONS



E. Method to Calculate Maximum Boulder Size

Determining the largest boulder size is critical for designing both the overflow and permeable sections of the dam, as well as calculating the impact load for the structure, per the Technical Guideline for Designing Sabo Facilities. Over 200 boulders within 200 meters upstream and downstream of the dam site are measured to create a frequency distribution of diameters. The 95th percentile of this distribution (D95) is deemed the maximum boulder size. Measurements are taken from boulder clusters on the riverbed, indicative of debris flow deposits. It's essential to ensure the D95 value accurately

Department/ Organization	Data Collected	Application
Department of Public Works and Highways (DPWH)	RIDF (San Agustin, Arayat Station)	Hydrologic Analysis
	Design Guidelines, Criteria, and Standards (Volume 3)	Hydrologic Analysis
	Proposed Debris Flow Barriers Plan	Hydraulic Analysis
	Bearing Capacity Analysis	Design
Mines and Geosciences Bureau (MGB)	External Stability Against Bearing Capacity	External Stability Against Bearing Capacity
	Digital Elevation Model (DEM)	Hydrologic Analysis
	Watershed Boundary Shapefile of Mt. Arayat	Hydrologic Analysis
	Debris Flow Hazard Assessment of Mt. Arayat	Hydrologic Analysis
	Landslide/Erosion Depth	RRL
	Debris Flow Hazard Map	Debris Transport Analysis
Pampanga River Basin Flood Forecasting and Warning Center (PRFFWC)	Delineation of Debris Flow	Delineation of Debris Flow
	Rainfall Data of Typhoon Santi (October 2013)	Hydrologic Analysis
	Compendium of Annual Hydrological Data Summaries (2009-2020)	Hydraulic Analysis
Pampanga Provincial Disaster Risk Reduction and Management Office	Annual Report 2013 (Programs, Activities, and Accomplishments)	Hydrologic Analysis
	Landslide Hazard Map	RRL

Resources (DENR), delineated the debris flow on Mt. Arayat after Typhoon Karding in 2022. Their debris flow hazard map (Figure 8) shows active and inactive debris flow channels, with most creeks identified as active.

Fig. 8 Debris Flow Hazard Map of SapangMaeyagas Creek, Mount Arayat National Park and Vicinity

To protect San Juan Baño's population and properties, SapangMaeyagas Creek is the optimal path for a Sabo Dam. The Department of Public Works and Highways (DPWH) - Region III proposed debris flow barriers in SapangMaeyagas Creek. This study complements DPWH's plans, using their proposed locations for Sabo Dams, as the DPWH project is yet to be implemented. Figure 9 shows the two proposed Sabo Dam locations along SapangMaeyagas Creek. The Diversion Creek intervention was excluded as it poses no downstream risk.

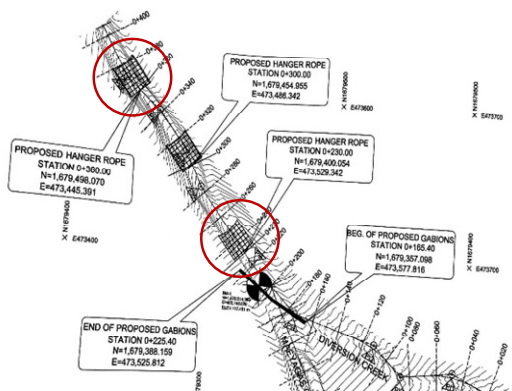


Fig. 9 Location of Engineering Interventions along SapangMaeyagas Creek and Diversion Creek by DPWH [19]

G. Data Analysis

Geotechnical Analysis

In this study, a geotechnical examination focused on assessing the characteristics of soil and rock, including parameters such as average grain size and internal friction angle. The purpose of this

evaluation was to provide insights for the design of foundations and various structures that interact with the ground. This phase was essential for conducting analyses related to debris transport and for the design process of the Sabo Dam.

Mean Grain Diameter (D50)

The mean grain diameter, serving as an indicator of the average size of soil particles, played a key role in soil classification and characterization, particularly in the analysis of debris transport. Within the framework of the Sabo Dam study, it was employed in the iRIC software to predict the

movement of sediment and debris during hydraulic events. This utilization facilitated the design of effective measures for debris control. Understanding the mean grain diameter was essential for discerning the sizes of boulders and debris at the site, thereby ensuring the dam's resilience against transported materials during periods of high flow.

The mean grain diameter can be computed by taking the sum of the diameters of a sample of boulders and then dividing by the number of boulders. The formula is as follows:

$$\bar{D} = \frac{\sum_{i=1}^n D_i}{n}$$

where D_i represents the diameter of each individual boulder. The location of the study area is shown in the map, highlighting Sapang Maeyagas Creek and Diversion Creek in San Juan, Baño, Arayat, Province of Pampanga. The hazards identified include Debris Flow, San Juan Baño a "depositional zone", and Rock Slides deposit brought by previous and recent typhoons. The analysis focuses on the soil slope resilience referred to structural angle and stability of the dam's slopes and foundation [20].



Location: Sapang Maeyagas Creek and Diversion Creek, San Juan, Baño, Arayat, Province of Pampanga

- Hazards:
- Debris Flow
 - San Juan Baño a "depositional zone"
 - Rock Slides deposit brought by previous and recent typhoons

TABLE II
TYPICAL VALUES OF SOIL FRICTION ANGLE

Landform	Lag Time Coefficient (Ct)
Mountainous Area	1.20
Hilly Area	0.70
Valley Area	0.35

Hydrologic Analysis

The hydrologic analysis in this study was conducted using the HEC-HMS (Hydrologic Engineering Center's Hydrologic Modeling System) software, a widely utilized tool for simulating the rainfall-runoff processes of watershed systems. The model's accuracy and reliability were ensured through calibration with observed data. Subsequently, the calibrated model was employed to generate hydrographs, which graphically represent the flow rate of water over time at specific locations.

Data Inputs

- Terrain Data: Digital Elevation Model (DEM) rasters were prepared using QGIS, an open-source software for geospatial data.
- Rainfall Data: Processed in the meteorologic model using a specified hyetograph method.
- Rainfall Intensity Duration Frequency (RIDF) Data: Processed using the frequency storm method.

Model Components

Runoff processes were simulated using various models in HEC-HMS. Direct runoff/transform models simulated surface water movement, while baseflow models were omitted due to the ephemeral nature of the creek. Routing models simulated channel flow using the Muskingum method for stream channel routing. Additionally, the SCS Unit Hydrograph was used as the transform method to determine peak discharge rates [9].

To determine peak discharge rates, the SCS unit hydrograph was used as the transform method, as

Well g
Poorly
Silty
Clayey
Loam
Inorga
san

recommended by DPWH. The Muskingum method for routing involves K (travel time), X (attenuation coefficient), and the number of subreaches, estimated through manual calibration due to a lack of observed discharge data [21].

Lag time, the delay between maximum rainfall and peak discharge, was calculated using a modified version of Snyder's Lag Equation, suitable for studies in the Philippines. This approach helped address relevant hydrological considerations for the watershed under study[22, 23].

$$Lg = 0.6865 \times Ct \times \left[\frac{L \times Lca}{\sqrt{S}} \right]^{-0.38}$$

H.

Where:

Lg: Lag time (hour)

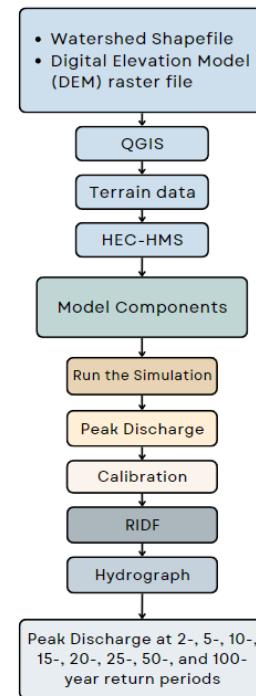
Ct: Lag time coefficient

TABLE III
VALUES FOR LAG TIME COEFFICIENT

L : length of water course from the downstream end of the subbasin to the upstream sub-basin boundary (km)

Lca : length of water course from the downstream end of the subbasin to a intersection on the stream perpendicular from the centroid of the subbasin (km)

S : average basin slope (overall slope along longest water course from the downstream to upstream ends of the subbasin)



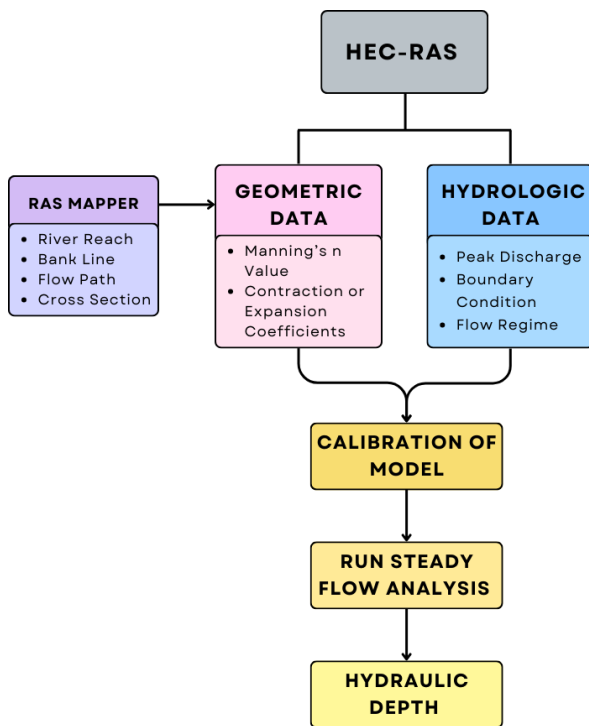


Fig. 10 Flowchart of HEC-HMS Simulation

Model Calibration and Simulations

After gathering all required input data and selecting models for each basin, the HEC-HMS model underwent calibration to ensure accurate outputs. The model was then prepared to simulate different return periods, ranging from 2 to 100 years using RIDF data. To establish the frequency storm duration for model application, the time of concentration (tc) was calculated using techniques such as Kirpich's Formula and Kraven's Formula[24].

I. Hydraulic Analysis

In this study, the hydraulic analysis was performed using the HEC-RAS software, employing a steady flow model based on the one-dimensional energy equation. The analysis assumed a steady, gradually varied flow within the channel.

The HEC-RAS 1D flow model geometry, including the river network and cross-sections, was developed using the Ras Mapper extension within the HEC-RAS software. This geometry was based on the Digital Elevation Model (DEM) provided by

the Mines and Geosciences Bureau. Accurate representation of the channel geometry and terrain was ensured by integrating the high-resolution DEM data.

Peak discharge values derived from the Hydrologic Modeling System (HMS) simulations were input into the RAS model for hydraulic simulations. Boundary conditions were specified at either the upstream or downstream ends of the model, depending on the flow regime and the specific requirements of the simulation.

Additional calibration steps were performed to ensure the reliability and accuracy of the model. These steps included comparing simulated water surface elevations with observed data. Figure 11 illustrates the steps involved in conducting the hydraulic analysis using the HEC-RAS software [25].

Fig. 11 Flowchart of HEC-RAS Simulation

J. Debris Transport Analysis

For debris flow simulation to be user-friendly and effective, it needs an easy-to-use interface (GUI) that helps users visualize information and run simulations without requiring expert knowledge. This visualization allows users to easily grasp data such as water discharge, flow depth, and debris thickness. An example of such a tool is Morpho2DH, developed by Hiroshi Takebayashi at Kyoto University. Morpho2DH is a dynamic, two-dimensional flow and morphodynamics solver designed specifically for analyzing debris and mud flows, expanding on the Morpho2D model used for water flows.

Figure 12 illustrates the stages of simulation using iRIC Morpho2DH. This tool accurately simulates the transportation and deposition of debris by landslides, including erosion of the riverbed and banks. Morpho2DH stands out in the iRIC suite for its ability to predict mud and debris flows. It also includes features for adding closed

type Sabo Dams and obstacles, enabling predictions of flow paths even in complex urban areas. However, Morpho2DH has some limitations. It assumes that sediment concentration remains constant over time and space, simplifying material behavior and potentially not fully capturing changes in water and sediment content, thereby affecting local flow properties. Despite these limitations, Morpho2DH has demonstrated its ability to accurately predict flow depth, which is crucial for risk assessment [26].

Fig. 12 Flowchart of iRIC Simulation

K. External Stability Analysis

The concept of safety performance in relation to a Sabo Dam encompasses maintaining the integrity of external stability which includes considerations of overturning, sliding, and bearing capacity. An academic paper titled Technical Standards and Guidelines for Planning and Design of Sabo Structures by JICA served as the premise to carry out the External Stability Analysis [27].

Stability Calculation Against Overturning and Tensile Stress

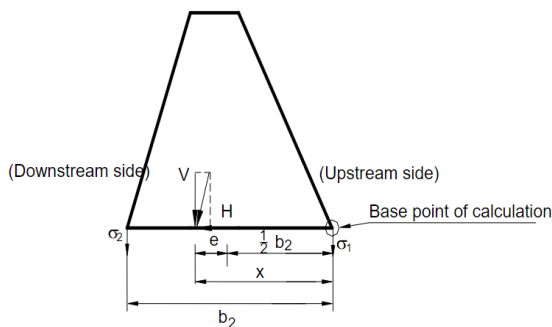
$$X = \frac{M}{V}$$

Where:

- X = Length between the point of working resultant force at dam bottom and upstream end (m)
- M = Sum of the overturning moments at the upstream end (kN-m)

For the stability against overturning, the value shall be satisfied:

$$\frac{b_2}{3} \leq X \leq \frac{2b_2}{3}$$



A. Text Font of Entire Document

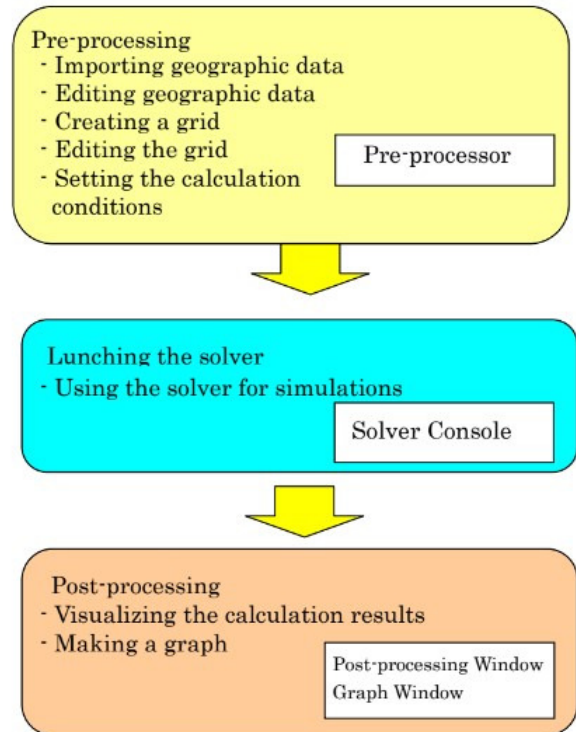
Fig. 13 Working Force on Typical Cross Section

Stability Calculation Against Sliding

$$F_s = \frac{fV + \tau \ell}{H}$$

Where:

- F_s = Safety factor against sliding ($F_s > 4.0$ or 1.2)



- V = sum of normal force per unit width (kN/m)
- H = sum of shearing force per unit width (kN/m)
- f = Coefficient of internal friction at the contact plane
- τ = Unit shear strength which is the smaller value of either the foundation or its contact plane with concrete (kN/m²)
- ℓ = Length of shear resistance in embedment (m)

In case the dam height is less than 15m, the safety value of F_s shall be 4.0 for bedrock, and 1.2

for sand and gravel. The value of F (1.2) for sand and gravel foundation shall be calculated to neglect the shear strength.

Stability Checking Against Bearing Capacity of Ground

Every normal stress must remain below the permissible load-bearing capacity as determined by the ground's material type.

$$Q = \frac{V}{b_2} \left(1 \pm \frac{6e}{b_2}\right)$$

$$e = X - \frac{b_2}{2}$$

TABLE IIIV
ALLOWABLE BEARING CAPACITY OF FOUNDATION

ALLOWABLE BEARING CAPACITY OF SOIL (kPa)						
Depth m	B _{f1} 1	B _{f2} 2	B _{f3} 3	B _{f4} 4	B _{f5} 5	B _{f6} 6
1.50	68	68	69	70	70	71
3.00	250	254	258	261	265	268
4.50	230	234	237	241	244	248
6.00	321	325	329	332	336	339
7.50	357	360	364	368	371	375
9.00	336	340	344	347	351	354
10.50	372	376	379	383	386	390
12.00	633	638	643	649	654	659
13.50	633	639	644	649	655	660
15.00	746	751	756	762	767	772

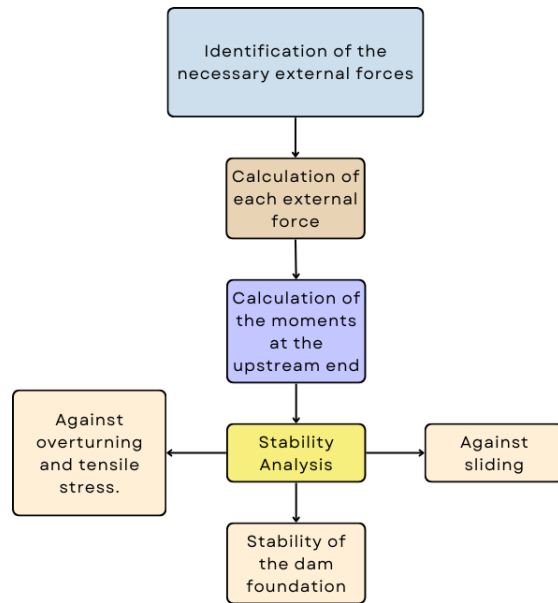


Fig. 14 Stability Analysis of Main Body

L. Design of Sabo Dam

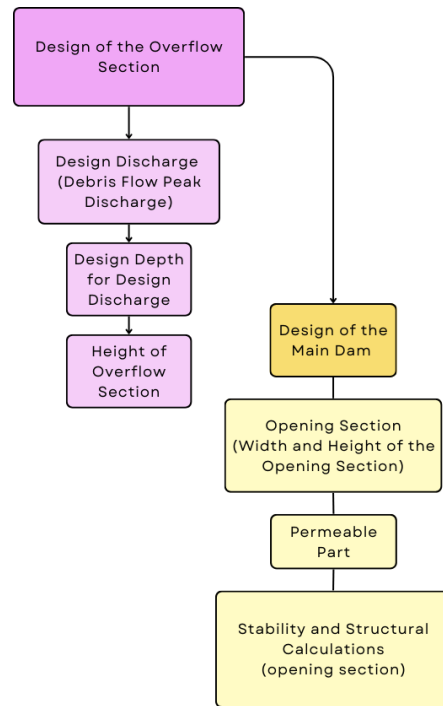


Fig. 15 Stability Analysis of Main Body

In Japan, the SABO (Erosion and Debris Control) Department of the Ministry of Construction (present Ministry of Land, Infrastructure, Transport

and Tourism) has made some laws and technical guidelines related to debris flows, shallow landslides caused by heavy rainfall, and deep-seated landslides [28].

The Technical Guideline for Designing Sabo Facilities against Debris Flows and Driftwood explains the methods of designing debris flow and driftwood facilities stipulated by the Sabo master plan against debris flow and driftwood created based on the Technical Guideline for Establishing Sabo Master Plan against Debris Flows and Driftwood.

**M. Structure of Open Type Sabo Dam
Stability of Overflow Section**

	Dam Height below 15 m	Dam Height Exceeding 15 m
ρ	11.8 kN/m ³	9.8 kN/m ³

For an open type Sabo Dam, it is crucial that the entire structure can withstand sliding, overturning, and sinking. Additionally, any permeable sections or other parts of the dam body must be able to resist debris flow. The design of an open type Sabo Dam should ensure that all components of the dam body, which are made up of different types of members, can withstand external forces as a single, integrated unit.

Design Discharge

The debris flow peak discharge utilized in designing the spillway section shall be regarded as the design discharge.

The peak discharge of debris flow is to be determined using the formula:

$$Q_{sp} = \frac{C *}{C * - C_d} Q'$$

Where:

Q_{sp} = Design peak discharge for debris flow (m³/s)

Q' = Design flood discharge (m³/s)

$C *$ = Volumetric sediment concentration of deposited sediment (about 0.6)

C_d = Volumetric sediment concentration of debris flow in motion (about 0.9C*).

Note: When riverbed gradient is greater than 20°, the concentration of debris flow can be estimated by the following equation:

$$C_d = \frac{\rho \tan \theta}{(\sigma - \rho)(\tan \phi - \tan \theta)}$$

If the calculated value C_d is larger than 0.9C*, C_d shall be regarded as 0.9C*, and if it is smaller than 0.3, it shall be regarded as 0.30.

Where:

σ = Unit weight of boulder

ρ = Unit weight of water

ϕ = Angle of internal friction of deposited sediments

θ = Riverbed gradient

TABLE V
UNIT WEIGHT OF WATER

Design Water Depth

The depth of water at which the design discharge passes through the spillway is known as the design water depth, which also determines the overflow depth of the spillway.

The opening of Sabo dam is trapezoidal in shape following the principles below:

1. To avoid erosion of the dam downstream, the width of the crest opening (B_1) is expanded to its maximum feasible extent. The opening (B_1) should be a minimum of 3 meters wide to accommodate the passage of drifting wood and/or debris.

2. The height of the crest opening (H_c) is equivalent to the combined depth of flood discharge (h_1) and the freeboard (h_2).

$$H_c = h_1 + h_2$$

Depth of Debris Flow, h_1 :

$$h_1 = \frac{Q_{sp}}{B v_{df}}$$

Where:

h = Depth of debris flow (m)

Q_{sp} = Peak discharge of debris flow
(m^3/s)

B = Width of flow (m)

v_{df} = Velocity of debris flow (m/s)

Freeboard, h_2 :

$$Q = (1 + 0.5)Q'$$

Where:

Q = Design Discharge for Debris Flow
(m^3/s)

Q' = Design flood discharge (m^3/s)

TABLE VIV
PROPOSED FREEBOARD OPENING

Fig. 17 Cross-Section of a Spillway

The spillway must be wide enough to let the debris flow peak discharge pass through even if the permeable section is blocked by debris. In this scenario, the freeboard is not a concern. However, if there is not enough space for the flow in the spillway section due to topography or other factors, the wing section can be used as a flow section.

Setting of the Opening Section

The opening section of an open-type Sabo Dam must be sufficiently wide to ensure that it functions as a permeable structure.

- The height of the opening section should be equal to or greater than the depth of the debris flow or flood discharge bulked with debris, which is used to calculate the design capturing volume of debris flow.
- The design of the bottom surface of the

Proposed Discharge	Freeboard (m)
Below 200 m^3/sec	0.6
200 - 500 m^3/sec	0.8
500 m^3/sec or above	1.0

Height of opening shall be selected using the bigger height value between (i) and (ii)

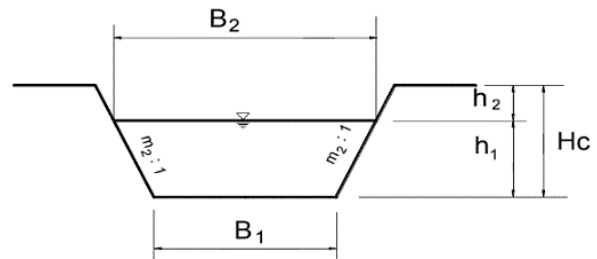
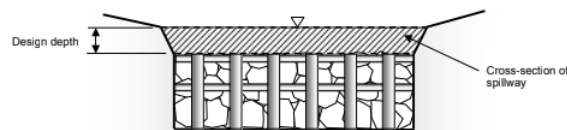
- Design depth + Freeboard
- Maximum diameter of boulder of debris flow (D_{95})

Fig. 16 Cross-section of Opening

Main Body Structure

Spillway Section

The section of the spillway should resemble that of a closed type Sabo dam, but it must be designed in a way that can safely handle the peak discharge of debris flow even if the permeable section is obstructed.



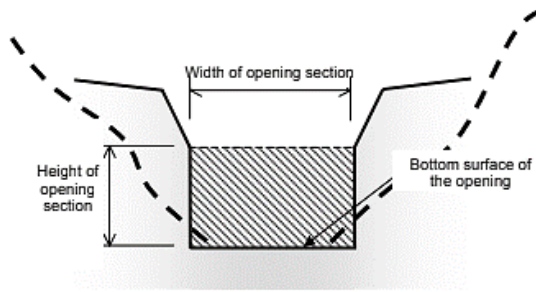


Fig. 18 Opening section of an open type Sabo Dam

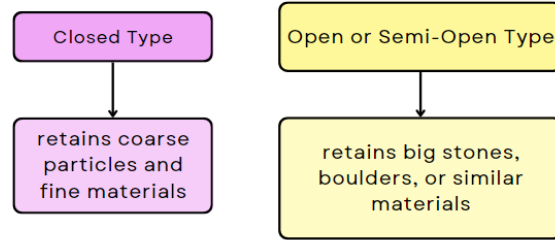


Fig. 20 According to the Debris Retained

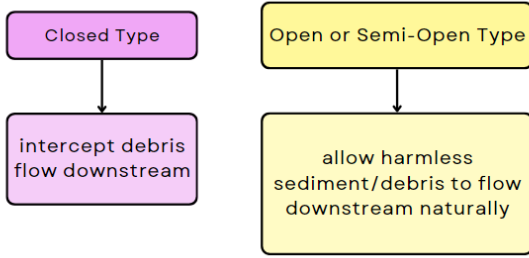


Fig. 21 According to the Process of Debris Flow

to be obstructed by the debris flow that follows, and this blockage continues throughout the latter part of the debris flow.

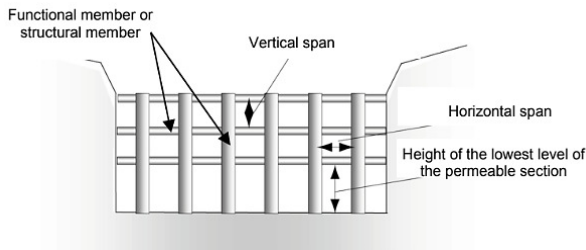


Fig. 19 Span of Permeable Section

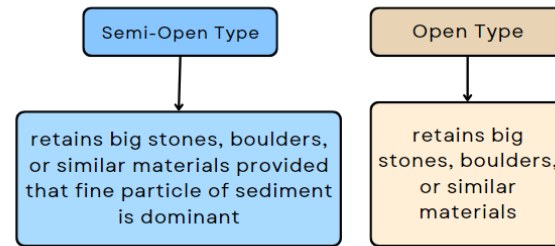


Fig. 22 Main Difference between Semi-Open Type and Open-Type Sabo

III. RESULTS AND DISCUSSION

A. Determination of the Type of Sabo Dam

Therefore, based on the above statements and the revision made in the Technical Guideline for Designing Sabo Facilities against Debris Flows and Driftwood, the type of Sabo Dam that must be adopted in this study in line with the requirements of the study area is an Open-Type Sabo Dam.

B. Geotechnical Analysis Mean Grain Diameter

Table VII below shows the diameters, in centimeters, of 200 boulders measured at the site where the Sabo Dam is planned to be designed.

TABLE VIV
DIAMETERS OF 200 BOULDERS SAMPLED

34	63	71	80	86	95	106	116	126	144
35	63	72	80	87	96	107	116	127	144
38	63	72	80	87	96	107	117	128	144
39	64	73	80	87	97	107	117	128	145
42	64	73	82	87	97	107	117	128	147
43	64	73	82	88	97	108	117	128	148
43	65	73	83	88	97	108	118	130	148
46	66	75	83	88	97	108	118	130	150
48	67	76	83	90	98	108	120	132	152
48	67	76	83	90	99	109	120	133	152
49	67	77	84	90	100	109	120	133	152
52	68	77	84	92	103	110	121	134	153
57	68	78	84	93	103	110	121	134	153
59	69	78	84	93	103	111	122	134	155
61	70	78	84	93	104	112	123	134	155
61	70	78	85	93	104	113	123	136	157
62	70	79	85	94	104	114	124	136	157
62	70	79	85	94	105	114	124	136	157
62	70	79	85	94	105	114	125	136	160
63	70	80	86	95	105	115	125	140	161

Using the data on boulder sizes, the mean grain diameter has been calculated to be 98.065 centimeters, which is equivalent to 0.98065 meters.

$$\bar{D} = \frac{\sum_{i=1}^n D_i}{n}$$

$$\bar{D} = \frac{19613cm}{200}$$

$$\bar{D} = 98.065cm$$

Determining the mean grain diameter is a critical step in the design phase of the Sabo Dam, as it provides valuable information about the average size of the boulders present at the site. This information is essential to assess the suitability of the materials and ensure the stability and effectiveness of the dam structure.

Internal Friction Angle

The soil type in Arayat is sandy clay loam, which is a soil composition containing 45 to 80% sand, 20 to 35% clay, and 0 to 28% silt. This type of soil offers a balance between the drainage properties of

sandy soils and the nutrient-retaining properties of clay soils.

For sandy clay loam, the internal friction angle, a critical parameter in geotechnical engineering, typically ranges from 31 to 34 degrees, as indicated in Table VIII. The internal friction angle is a measure of the shear strength of the soil and influences how the soil resists sliding along internal planes. While the friction angle for sandy clay loam can vary, 34 degrees represents the maximum value, indicating the highest shear strength this soil type can achieve under optimal conditions.

TABLE VIIIVI
TYPICAL VALUES OF SOIL FRICTION ANGLE

Description	USCS	Soil friction angle [°]	
		min	max
Well graded gravel, sandy gravel, with little or no fines	GW	33	40
Poorly graded gravel, sandy gravel, with little or no fines	GP	32	44
Sandy gravels - Loose	(GW, GP)		
Sandy gravels - Dense	(GW, GP)		
Silty gravels, silty sandy gravels	GM	30	40
Clayey gravels, clayey sandy gravels	GC	28	35
Sand	SW, SP	37	38
Silty sands	SM	32	35
Loamy sand, sandy clay Loam	SM, SC	31	34
Inorganic silts, silty or clayey fine sands, with slight plasticity	ML	27	41

C. Hydrologic Analysis

Hydrological simulations, especially with HEC-HMS, are crucial for water resource management, aiding in infrastructure design and hazard prediction. In this study, HEC-HMS simulated return periods from 2 to 100 years, focusing on the 100-year period to determine peak discharge for designing hydraulic structures.

Physical Conditions of Sub-basins

TABLE VIIIX
CATCHMENT AREA AND LAG TIME OF SUB-BASINS

Subbasin	Catchment Area (sq.km)	Length (km)	Slope S	Lca (km)	Ct
S-1	0.2204	0.6298	0.68514	0.31714	1.2
S-2	0.3618	1.95945	0.27763	1.18911	1.2
S-3	0.1435	0.45933	0.69448	0.25142	1.2
S-4	0.1628	0.9476	0.16463	0.40318	0.7
S-5	0.1633	0.44952	0.70075	0.16458	1.2

Table IX provides an analysis of areas and lag individual sub-the Maeyagas model. Seven sub-identified, with a cumulative catchment area of 1.4541 km², offering insights into spatial water source distribution.

Lg	
(hr)	(min)
0.47995013	28.79701
1.449300812	86.95805
0.388745878	23.32475
0.469687506	28.18125
0.327667001	19.66002
0.564583344	33.875
0.532531862	31.95191

provides an analysis of areas and lag individual sub-the Maeyagas model. Seven sub-identified, with a cumulative catchment area of 1.4541 km², offering insights into spatial water source distribution.

Calibration of HEC-HMS Model

In routing modeling for the Maeyagas Creek basin, the Muskingum method divides the watershed into three reaches, each with calibrated parameters: Muskingum K values represent traverse times for each reach, with values of 0.08 hours, 0.20 hours, and 0.31 hours for reaches 1, 2, and 3, respectively. A uniform X value of 0.07 across all reaches indicates significant flow slowing. During calibration, the HEC-HMS model utilized data from the Arayat Rainfall Station, including the maximum 24-hour rainfall rate of 0.22 meters recorded during Typhoon Santi on October 11, 2013, with a recurrence interval of 2 years, aiming to accurately simulate real-world hydrological conditions. The hydrograph generated by the model exhibited a peak discharge of 5.9 m³/s, aligning precisely with a depth of 0.22m in the HEC-RAS software, indicating the effectiveness of the calibration process.

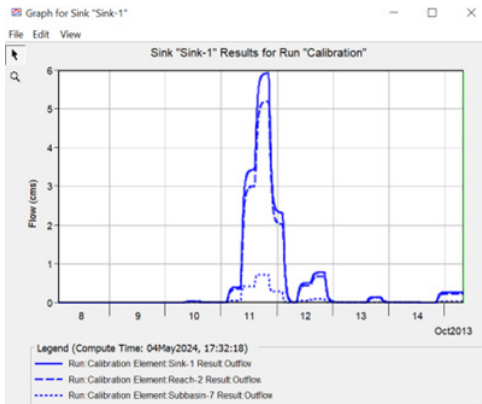


Fig. 23 Flood Hydrograph of the Calibration

Peak Discharge with 100-Year Return Period

The tc value of 34.024 minutes, obtained from Kirpich's formula, is used to determine the storm duration frequency for model application. Sink 1 recorded a peak discharge of 31.4 m³/s for the 100-year return period. This data guided the design of sabo dam infrastructure to withstand and mitigate the effects of rare but severe flood events, protecting downstream communities and the environment. Figure 42 illustrates the flood hydrograph associated with Sink 1 for this return period.

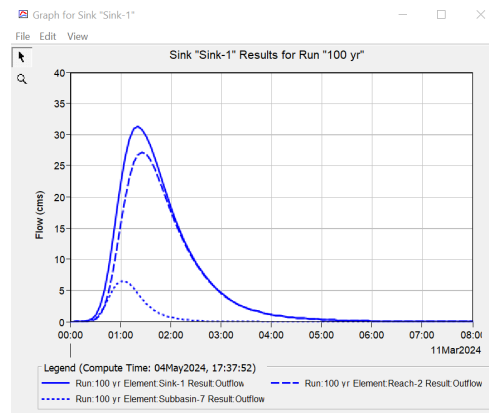


Fig. 24 Flood Hydrograph of the Watershed based on 100-Year Return Period

D. Hydraulic Analysis

Manning's Roughness Coefficient (n)

In the hydraulic model, the calibration process primarily focused on determining the manning's roughness coefficient value, a crucial parameter influencing flow characteristics within the channel.

Typical ranges of roughness values for different channel types were referenced from the DPWH Design Guidelines, Criteria, and Standards Volume 3 for Water Engineering Projects, as well as Chow (1959). These guidelines suggest that Manning's n values between 0.05 and 0.07 are suitable for mountain streams characterized by no vegetation in the channel, steep banks, and a bottom composed of cobbles with large boulders.

During the model runs, various Manning's n values within this range were tested to determine the most appropriate value for the main channel and the overbank areas. Following thorough testing and

calibration, a Manning's n value of 0.07 was selected for the main channel, with corresponding values of 0.07 for both the left and right overbank areas as shown in Figure 25. This value indicates a moderately rough channel surface, reflecting the presence of large boulders and cobbles that contribute to flow resistance.

Manning's n Values		
LOB	Channel	ROB
0.07	0.07	0.07

Fig. 25Manning's Roughness Coefficient for Calibration of Model

Calibrated Hydraulic Depth

The hydraulic model was calibrated to ensure its accuracy in simulating flow conditions within the channel. This involved comparing the model's simulated water depth with the actual depth observed during a significant rainfall event, specifically Typhoon Santi's peak rainfall in 2013. The observed water depth during this event was 0.22 meters, closely matching the depth predicted by the model. This alignment indicates the model's effectiveness in representing the channel's hydraulic behavior during peak flow conditions. With successful calibration, the model's parameters were deemed appropriate and retained for subsequent simulations. Figure 26 displays the cross-sectional output generated during calibration, visually confirming the model's ability to replicate observed hydraulic conditions. This output validates the model's accuracy and reliability in simulating flow depths within the channel.

Element	Left OB	Channel	Right OB
Wt. n-Val.		0.070	
Reach Len. (m)	1.82	1.78	1.77
Flow Area (m ²)		2.85	
Area (m ²)		2.85	
Flow (m ³ /s)		5.90	
Top Width (m)		12.93	
Avg. Vel. (m/s)		2.07	
Hydr. Depth (m)		0.22	
Conv. (m ³ /s)		14.8	
Wetted Per. (m)		12.98	
Shear (N/m ²)		340.39	
Stream Power (N/m s)		703.84	
Cum Volume (1000 m ³)	0.05	0.55	0.01
Cum SA (1000 m ²)	0.34	2.71	0.15

Fig. 26Cross Section Output of Calibration

Cross-Sectional Output at Station 234

The results from the HEC-RAS simulation conducted at station 234, utilizing the discharge associated with the 100-year return period derived from the HEC-HMS output, provide significant

insights into the hydraulic conditions at the proposed site for the Sabo Dam.

The calculated hydraulic depth of 0.52 depicted in Figure 27 indicates that the flow within the creek is relatively shallow. This depth is constrained by the ephemeral nature of the creek, which means that water flow occurs only during certain periods, usually after rainfall events. It is important to note that the location being in a mountainous area further affects water flow dynamics, as water does not tend to accumulate significantly due to the terrain.

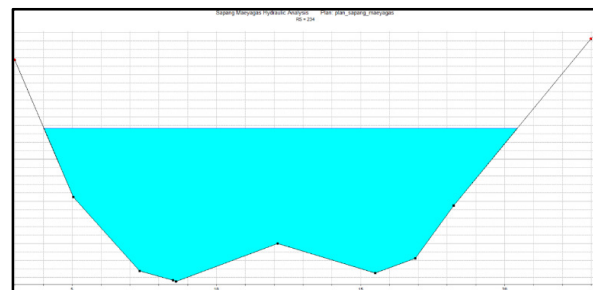
Element	Left OB	Channel	Right OB
Wt. n-Val.		0.070	
Reach Len. (m)	1.82	1.78	1.77
Flow Area (m ²)		8.48	
Area (m ²)		8.48	
Flow (m ³ /s)		31.40	
Top Width (m)		16.41	
Avg. Vel. (m/s)		3.70	
Hydr. Depth (m)		0.52	
Conv. (m ³ /s)		77.6	
Wetted Per. (m)		16.56	
Shear (N/m ²)		822.96	
Stream Power (N/m s)		3046.57	
Cum Volume (1000 m ³)	0.23	1.52	0.14
Cum SA (1000 m ²)	0.83	3.19	0.75

Fig. 27Cross Section Output based on 100-Year Return Period Discharge

In Figure 28, the cross-section illustrates the designated location for the proposed Sabo dam at 15°11'19.4"N 120°45'03.7"E. The maximum channel depth observed is 0.73 meters. However, the study focused on utilizing hydraulic depth rather than the maximum channel depth. Hydraulic depth, calculated as the flow area divided by the top width, accommodates the altered channel geometry resulting from dam construction activities.

Fig. 28Cross Section at Station 234

E. Debris Transport Analysis



In this study, the Morpho2DH solver of iRIC was utilized to model a debris flow occurring in SapangMaeyagas Creek. The main goal of this

study was to determine the maximum depth and width of the debris flow in meters, while also capturing the velocity of the debris flow in meters per second.

Calculation Parameters

In the Morpho2DH solver, several key parameters have been established for accurate modeling of debris flow dynamics in the SapangMaeyagas creek. The maximum erosion depth is set at 1.5 meters, reflecting observed debris flow heights. A mean grain diameter of 0.981 meters was determined through surveying. Manning's roughness coefficient is fixed at 0.07, derived from calibrated parameters of the HEC-RAS software. The discharge obtained from hydrological analysis, 31.4 cubic meters per second, serves as a boundary condition.

Given the focus on Sabo Dam design, the calculation type is specified as debris flow, necessitating the inclusion of crucial parameters. The static deposition sediment concentration is set at 0.6, chosen within the solver manual's recommended range. The liquid behaviors ratio is established as 0.2, standard for finer sediment diameters. The minimum flow depth is determined by the smallest surveyed boulder size, 0.34 meters.

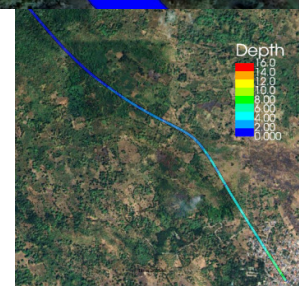
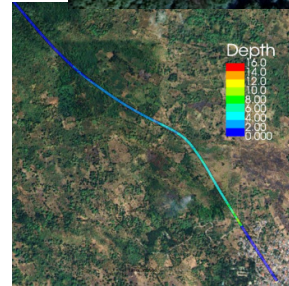
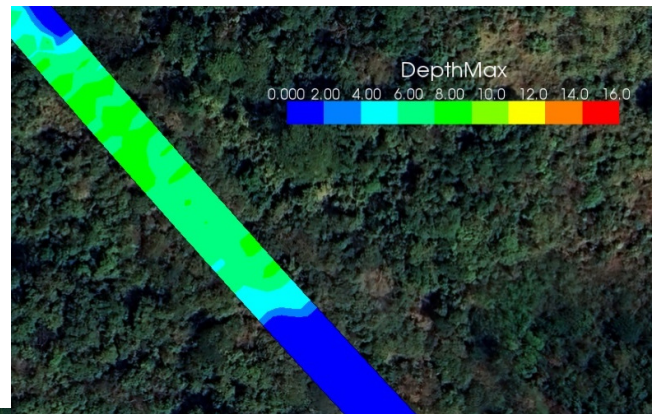
Considering the prevalent sandy clay loam soil type, an internal friction angle of 34 degrees is adopted to align with the mechanical properties of the soil and enhance simulation accuracy. Detailed calculation conditions are outlined in Table X, following specifications from the technical report on the Morpho2DH solver.

TABLE X
CALCULATION PARAMETERS OF THE MORPHO2DH

Calculation Type	DebrisFlow
Static Deposition Sediment Concentration	0.6
Liquid Behavior Sediment Ratio	0.2
Minimum Flow Depth	0.42 m

Internal Friction Angle	34 degrees
Laminar Flow Depth	Change
Resistance Coefficient	72

IRIC Simulation Without Sabo Dam In the simul



(3)

(4)

ation without the Sabo Dam, at time 240 seconds, the debris flow reached the residential area. Figure 29 visually represented the spatiotemporal evolution of debris flow depth. Initially, the debris flow masses were minimal, but they progressively grew over time due to the addition of eroded bed material and water.

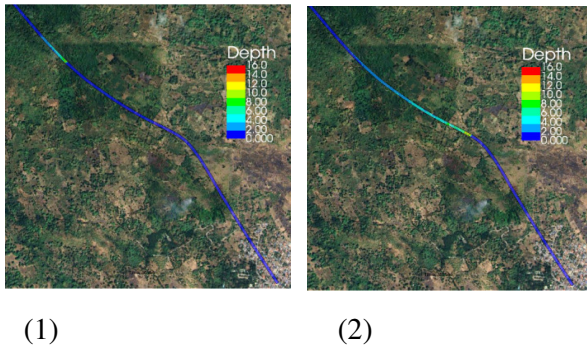


Fig. 29 Spatiotemporal variations in debris flow depth. (1), (2), (3), and (4), represents the flow depth at 60 s, 120 s, 180 s, and 240 s, respectively

Maximum Depth, Velocity and Width of Debris Flow

Based on the simulation results, it was observed that the maximum depth of the debris flow at the designated site for the Sabo Dam reached approximately 7.94 meters, with a corresponding velocity of 5.6 meters per second. Additionally, the width, determined through flow measurement, was found to be 20 meters. These findings are of utmost importance in the design phase of the Sabo Dam, as they provide critical insights into the required dimensions and specifications necessary to effectively mitigate the impact of debris flow. Figure 30 visually represents the results obtained from the iRIC calculations, offering a clear depiction of the simulated data for further analysis and decision-making in the dam design process.

Attributes:		
	Attribute Name	Value
1	Depth	7.93990064186...
2	DepthMax	7.93990064186...
3	Elevation	372.663202870...
4	IBC	1
5	WaterSurfaceEl...	380.603103512...
6	ElevationChange	-1.33679712923...
7	MeanGrainSize	0.98099999999...
8	FrictionVelocity	0.82823117194...
9	BedShearStress	0.04319974369...
10	VelocityX	3.73812270994...
11	VelocityY	-4.16300051110...
12	Velocity (magni...	5.59500979892...

Fig. 30 Results of iRIC Simulations

iRIC Simulation with Sabo Dam

In the simulation featuring the Sabo Dam, depicted in Figure 31, the debris flow reached the dam at 43 seconds into the simulation. The Sabo Dam is located 300 meters from the designated landslide area in the software. The dam implemented in the simulation is a closed-type Sabo Dam, as it was the only type considered by the software. The dimensions of the Sabo Dam were determined through iterative testing in the simulation. It was found that with a height of 8 meters, the dam effectively halted the progression of the debris flow.

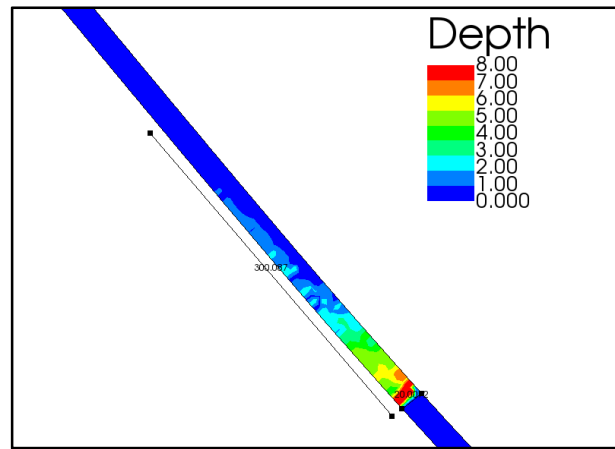


Fig. 31 Simulation with Sabo Dam

F. Design of Sabo Dam

The forces acting on the Sabo Dam were determined using guidelines for erosion and sediment control in mountainous regions, with adjustments to suit the study's requirements. A key modification was including forces from flowing water or hydrostatic pressures, crucial for accurately assessing the dam's stability.

This inclusion was driven by the creek-like characteristics of the area, where flowing water impacts debris movement, especially during the rainy season. This underscores the importance of considering hydrostatic forces in hazard assessment and mitigation design.

The study focused on the steel section of the Sabo Dam but also assessed the stability of the concrete

sections to ensure a comprehensive evaluation of the entire structure.

TABLE XI
RESULTS OF STABILITY ANALYSIS FOR THE STEEL AND CONCRETE SECTIONS OF THE OPEN TYPE SABO DAM

Failure Mode	Steel Section	Concrete Section
Overturning	$e = 7.573$ $4.633 < 7.573 < 9.267$	$e = 7.268$ $4.633 < 7.268 < 9.267$
Sliding	$7.296 > 4$	$11.686 > 4$
Bearing Capacity	$Q_1 = 166.311$ $< 268 \text{ kN/m}^2$ $Q_2 = 95.862$ $> 0 \text{ kN/m}^2$	$Q_1 = 267.348$ $< 268 \text{ kN/m}^2$ $Q_2 = 202.770$ $> 0 \text{ kN/m}^2$

As shown on Table XI, both of the steel and concrete sections of the open type Sabo dam have satisfied the conditions to conclude that the structure is safe against the three different modes of failure.

The factors taken into account during the analysis of debris flow included the self-weight of the steel pipes forming the core structure of the Sabo Dam, the weight of the debris flow, earth pressure, and hydrostatic force.

Excel was utilized for manual computation of these loads. These forces play a crucial role in verifying the external stability and safety of the Sabo Dam against three potential failure modes: overturning, sliding, and bearing capacity failure. It is essential for the vertical and horizontal forces, along with their resulting moments, to complement

resulting horizontal forces to prevent overturning and sliding, while also remaining within allowable bearing capacity limits to avoid excessive settlement.

Fig. 32 Elevation of Sabo Dam

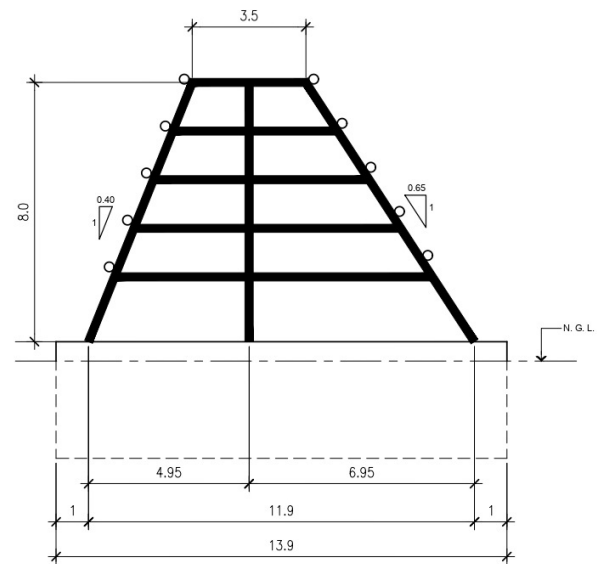
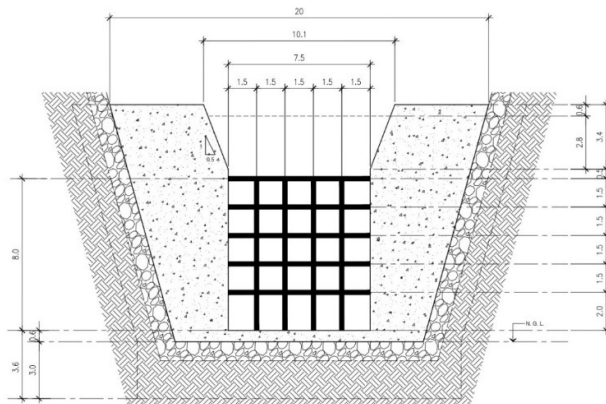


Fig. 33 Sabo Dam Steel Section



each other to prevent these failures. Specifically, the sum of vertical forces must significantly exceed

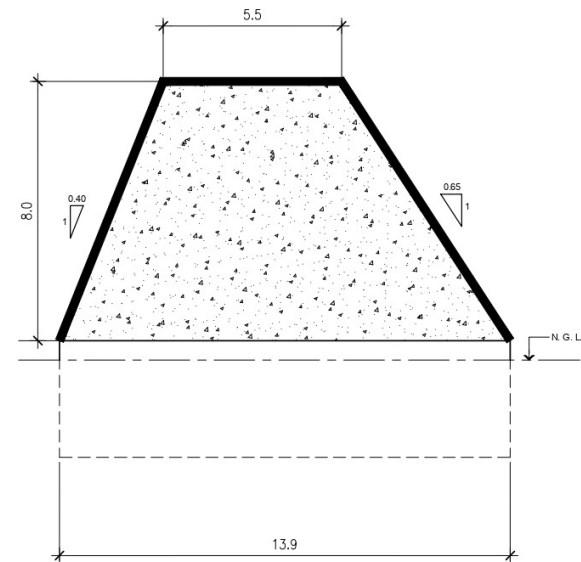


Fig. 34 Sabo Dam Concrete Section



Fig. 35 Location of Sabo Dam

III. CONCLUSIONS

A. Conclusion

Based on the findings of the study, the researchers were able to determine the exact location of the designed Sabo Dam at 15°11'19.4"N 120°45'03.7"E. Using data on the delineation of debris flow from MGB and DPWH, and utilizing various software tools, the appropriate design considerations were identified. HEC-HMS was used to determine the peak discharge rate, HEC-RAS was employed to determine the hydraulic depth, and iRIC was used to determine both the maximum depth and the width of the debris flow along with the corresponding velocity. The design of the Sabo Dam meets the necessary conditions for probable failure modes in external stability, specifically stability against shearing, overturning, and soil bearing capacity.

B. Summary of Findings

TABLE X
SUMMARY OF FINDINGS

Hydrologic Analysis		Peak Discharge = 31.4 m ³ /s
Hydraulic Analysis		Hydraulic Depth = 0.52m
Debris Transport Analysis		Maximum Width of Debris Flow = 20m Maximum Height of Debris Flow = 8m Maximum Velocity of Debris Flow = 5.6m/s
Design	Steel Section	Vertical Steel Pipes: D _o = 400mm and D _i = 240mm
		Horizontal Steel Pipes: D _o = 300mm and D _i = 180mm
	Concrete Section	Top Width = 5.5m
		Bottom Width = 13.9m
	Overflow Section	H _c = 3.4m
	Foundation	Fdn = 3.0m (0.6m above NGL)
	Front Face Slope	0.40:1
	Back Face Slope	0.65:1
Foundation Extension	1m	
Location of Sabo Dam		15°11'19.4"N 120°45'03.7"E

C. Recommendations

Future researchers aiming to use this study as a foundation for their own work have multiple avenues for expansion.

- Since this study focuses on boulder analysis, future researchers must investigate other environmental aspects such as driftwood analysis.
- Future researchers can use the observed hydrograph in calibration processes to fine-tune hydrological models and improve the accuracy of predictions.
- In the pursuit of advancing our understanding and practical application of Sabo dams, future researchers must identify the threshold velocity of water flow required for optimal functionality of the Sabo Dam
- Future researchers must consider internal stability by utilizing Finite Element Analysis (FEA) for thorough examination and prediction of how structures or materials behave under various conditions.
- Future researchers should consider the design of a series of Sabo Dams to achieve a more comprehensive and effective approach to river management and flood control.

- Future research should focus on pile foundations for building Sabo dams.
- Future researchers can examine the cost-benefit analysis, considering the construction, maintenance, and long-term performance of the Sabo Dam.
- Future researchers must conduct a comprehensive survey within the study area to gauge the willingness of the affected community to permit the construction of a Sabo dam.
- Future researchers must determine if there will be debris transport within a 2-year return period and ascertain the diameter of boulders that can pass through the Sabo Dam.
- Future researchers may assess debris transport over return periods ranging from 2 to 50 years.
- Future researchers should ascertain the maximum volume of boulders that can be transported.
- Future researchers must determine the number of occurrences within a 100-year interval before the Sabo Dam reaches its capacity.
- According to the Mines and Geosciences Bureau, there are 70,000 cubic meters of debris present upstream that may be transported. Future researchers must identify how many instances this may occur and how many recurrences it is possible for the dam to accumulate that volume before the Sabo Dam acts solely as a weir.

These suggestions may guide future researchers as they expand upon this work, paving the way for new discoveries and a deeper understanding of the topic.

ACKNOWLEDGMENT

This study would not have been possible without the guidance and help of several individuals who contributed significantly to its completion. The researchers express their deepest gratitude to:

- Engr. Catherine G. Jaceldone, Engr. Aldrin Joseph M. Tadifa, and Engr. Tweety Ann A.

Salig (DPWH), Senior Geologist Ms. Ma Lourdes M. Cruz (MGB), PDRMO, and Mr. Hilton T. Hernando (PRFFWC-PAGASA) for their expertise and efficiency.

- Our research adviser, Engr. John Vincent G. Tongol, for his invaluable guidance, patience, and support.
- Our research coordinator, Engr. Raul O. Duya, for his contributions and insightful critiques.
- Our panelists, Engr. Inla Diana Salonga, Engr. Princess Kimberly S. Soriano, and Engr. Aaron S. Malonzo, for their constructive feedback.
- Capt. Froilan M. Soriano, Barangay Captain of San Juan Baño, Arayat, Pampanga, for his support and tour guidance.
- The Department of Science and Technology for their financial support.
- Ash Leonard S. Sanchez, Maximus P. Soriano, Jerwin B. Mamangun, Jericho Y. Reyes, Kate Catherine O. Ramos, Vince Joseph C. Sagum, Erika Samuel B. Solidum, and Jertrude P. Salunga for their support during data gathering.
- Our families for their unwavering love and encouragement.
- Our dearest God Almighty for giving us wisdom, courage, strength, and patience to finish our research study successfully.

REFERENCES

- [1] G. J. Atienza, "Projects: International Sabo Network," [sabo-int.org](https://sabo-int.org/projects/philippines.html). <https://sabo-int.org/projects/philippines.html> (accessed Oct. 16, 2023).
- [2] J. Huang, X. Li, L. Zhang, Y. Li, and P. Wang, "Risk perception and management of debris flow hazards in the upper salween valley region: Implications for disaster risk reduction in marginalized mountain communities," *International Journal of Disaster Risk Reduction*, vol. 51, p. 101856, Dec. 2020, doi: <https://doi.org/10.1016/j.ijdr.2020.101856>. Zhang, C. Zhu, J. K. O. Sin, and P. K. T. Mok, "A novel ultrathin elevated channel low-temperature poly-Si TFT," *IEEE Electron Device Lett.*, vol. 20, pp. 569–571, Nov. 1999.
- [3] T. Takahashi and D. K. Das, *Debris Flow: Mechanics, Prediction and Countermeasures*, 2nd edition. CRC Press, 2014. Accessed: Oct. 15, 2023. [Online]. Available: https://books.google.com.ph/books?hl=en&lr=&id=jSzMBQAAQBAJ&oi=fnd&pg=PP1&ots=Fizyjhnh&sig=8y7JtCo-KbL62GKdKTAp7eNrGE&redir_esc=y#v=onepage&q&f=false. E. Sorace, V. S. Reinhardt, and S. A. Vaughn, "High-speed digital-to-RF converter," U.S. Patent 5 668 842, Sept. 16, 1997.

- [4] Sabo Planning Division, "I S S N 1 3 4 6 -7 3 2 8 Technical Guideline for Designing Sabo Facilities against Debris Flow and Driftwood. National Institute for Land and Infrastructure Management Ministry of Land, Infrastructure, Transport and Tourism, Japan," 2022. Accessed: Nov. 13, 2023. [Online]. Available: <https://www.nilim.go.jp/lab/bcg/siryounn/tnn0905pdf/ks0905e.pdfM.Shell>. (2002) IEEEtran homepage on CTAN. [Online]. Available: <http://www.ctan.org/tex-archive/macros/latex/contrib/supported/IEEEtran/>
- [5] Sabo Planning Division, "I S S N 1 3 4 6 -7 3 2 8 Technical Guideline for Establishing Sabo Master Plan against Debris Flow and Driftwood. National Institute for Land and Infrastructure Management Ministry of Land, Infrastructure, Transport and Tourism, Japan," 2022. Accessed: Nov. 13, 2023. [Online]. Available: <https://www.nilim.go.jp/lab/bcg/siryounn/tnn0904pdf/ks0904e.pdf>
- [6] "7 Major Forces Acting on Gravity Dam | Components Of Dam," Oct. 20, 2020. <https://www.civilengineeringweb.com/2020/10/forces-acting-on-gravity-dam.html>
- [7] "Forces Acting on a Dam Structure and Calculations," The Constructor, Oct. 26, 2010. <https://theconstructor.org/water-resources/forces-acting-dam-structure/5251/>
- [8] S. He, W. Liu, and X. Li, "Prediction of impact force of debris flows based on distribution and size of particles," *Environmental Earth Sciences*, vol. 75, no. 4, Feb. 2016, doi: <https://doi.org/10.1007/s12665-015-5180-2>. Wireless LAN Medium Access Control (MAC) and Physical Layer (PHY) Specification, IEEE Std. 802.11, 1997.
- [9] Mines and Geosciences Bureau (2022), "DEBRIS FLOW HAZARDS ASSESSMENT OF THE MT. ARAYAT NATIONAL PARK MAGALANG AND ARAYAT, PROVINCE OF PAMPANGA."
- [10] G. M. A. News, "Residents worried over massive crack in Mt. Arayat," *GMA News Online*, Oct. 08, 2022. <https://www.gmanetwork.com/news/topstories/regions/847408/resident-s-worried-over-massive-crack-in-mt-arayat/story/> (accessed Oct. 26, 2023).
- [11] T. Orejas, "Rocks in Arayat creek threaten Pampanga folk," *INQUIRER.net*, Nov. 16, 2022. <https://newsinfo.inquirer.net/1693803/rocks-in-arayat-creek-threaten-pampanga-folk> (accessed Oct. 26, 2023).
- [12] T. Orejas, "DPWH allots P100 million to stop Arayat slides," *INQUIRER.net*, Nov. 23, 2022. <https://newsinfo.inquirer.net/1696616/dpwh-allots-p100m-to-stop-arayat>
- [13] "Rep. Gonzales asks DPWH, DENR to prevent landslides in Mt. Arayat - Journalnews," Nov. 02, 2022. <https://journalnews.com.ph/rep-gonzales-asks-dpwh-denr-to-prevent-landslides-in-mt-arayat/> (accessed Oct. 26, 2023).
- [14] "Delta gets P100M from DPWH vs Mt. Arayat rockslides - Pampanga News Now," *pampanganewsnow.com*, Nov. 21, 2022. <https://pampanganewsnow.com/delta-gets-p100m-from-dpwh-vs-mt-arayat-rockslides/> (accessed Oct. 26, 2023).
- [15] G. M. A. News, "Residents worried over massive crack in Mt. Arayat," *GMA News Online*, Oct. 08, 2022. <https://www.gmanetwork.com/news/topstories/regions/847408/resident-s-worried-over-massive-crack-in-mt-arayat/story/> (accessed Oct. 20, 2023).
- [16] Pineda Appeals to Stop Destructive Farming on Mountains – Provincial Government of Pampanga," *Pampanga.gov.ph*, 2022. <http://pampanga.gov.ph:82/news/index.php/pineda-appeals-to-stop-destructive-farming-on->
- [17] Holcim PH employees volunteer anew for envi initiatives," *www.holcim.ph*. <https://www.holcim.ph/news/latest-releases/latest-release/article/holcim-ph-employees-volunteer-anew-for-envi-initiatives?fbclid=IwAR1X9sfpDhD3ti3QSO4n1YVHenD47AUv4OZFd7ufi7FFn9RVDv2kgve9l6Y> (accessed Oct. 21, 2023).
- [18] DPWH, "Mt. Arayat, Pampanga Site Inspection for Debris Flow Barrier," Nov. 2022.
- [19] DPWH-Region III, "Flood Mitigation Structures Protecting Public Infrastructures/Facilities Rehabilitation of Slope Protection Structure at SapangMaeyagas, Brgy. San Juan Baño, Arayat, Pampanga"
- [20] GeotechData, "Angle of friction," *www.geotechdata.info*, 2013. <https://www.geotechdata.info/parameter/angle-of-friction>
- [21] "Applying the Muskingum Routing Method," *www.hec.usace.army.mil*. <https://www.hec.usace.army.mil/confluence/hmsdocs/hmsguides/apply-ing-reach-routing-methods-within-hec-hms/applying-the-muskingum-routing-method>
- [22] A. Stephenson, A. Farnum, and M. Horst, "Evaluating the Accuracy of the NRCS Lag Time Equation." Available: <https://fscollab.tcnj.edu/wp-content/uploads/sites/255/2020/09/Dr.-Michael-Horst-Austin-Farnum-Amanda-Stephenson-NRCS-Lag-Time-Poster-1.pdf>
- [23] "HECHMS Manual-All Fin," *pdfcoffee.com*. <https://pdfcoffee.com/hechms-manual-all-fin-pdf-free.html> (accessed Apr. 23, 2024).
- [24] "DGCS Volume 1 - DPWH," *Studocu*, 2018. <https://www.studocu.com/ph/document/far-eastern-university/bachelor-of-science-in-civil-engineering/dgcs-volume-1-dpwh/7154474> (accessed Nov. 10, 2023).
- [25] C. Horner, "Introduction to HEC-RAS," 2016. Available: https://www.engr.colostate.edu/~pierre/ce_old/classes/CIVE%20401/Guest%20Lectures%202016/Introduction%20to%20HEC-RAS.pdf
- [26] "Morpho2DH | Solvers | iRIC Software," *i-ric.org*. <https://i-ric.org/en/solvers/morpho2dh/> (accessed March 08, 2024).
- [27] "Manual Of Sabo Works.pdf | Powered by Box," *app.box.com*. https://app.box.com/s/3tbbnd9die?fbclid=IwZXh0bgNhZW0CMTEAAR3HK6Jpq9RAcurLINTzIaOqoArk4_q4oywqs9hq8qyWfGiYakSbKYaPK1o_aem_ARsG6dnAoN5FfiHEPZuvrv06Bj1Qt5DG6nzBT0A5Qv7oFwvIE2VN2zBp_qnIcJ_ibeUK8BRh9IA2WZvQ7j19Ey6p (accessed May 08, 2024).
- [28] S. Fadilah and D. Luknanto, "Effects of heavy rainfall on the slope stability – A case study on Imogiri Cemetery: The graveyard complex of Mataram Royal Kings," *E3S Web of Conferences*, vol. 200, p. 02006, 2020, doi: <https://doi.org/10.1051/e3sconf/202020002006>.